



ELSEVIER

Colloids and Surfaces A: Physicochem. Eng. Aspects 224 (2003) 207–212

COLLOIDS  
AND  
SURFACES

A

www.elsevier.com/locate/colsurfa

# Synthesis and characterization of titania-coated Mn–Zn ferrite nanoparticles

Ming Ma, Yu Zhang, Xiaobo Li, Degang Fu, Haiqian Zhang, Ning Gu\*

*National Laboratory of Molecular and Biomolecular Electronics, Southeast University, Nanjing 210096, China*

## Abstract

A novel core-shell structured composite, titania (TiO<sub>2</sub>) coated Mn–Zn ferrite nanoparticle, was prepared by hydrolysis of titanium (IV) chloride (TiCl<sub>4</sub>) in the presence of Mn–Zn ferrite nanoparticles synthesized with stearic acid gel method. The obtained samples were characterized by energy dispersive X-ray spectroscopy (SEM-EDS), X-ray diffraction (XRD) and transmission electron microscopy (TEM). Results show that spinel structural Mn–Zn ferrite nanoparticles (6 nm average diameter) or their aggregates are coated by TiO<sub>2</sub> nanoshell with anatase structure for annealed sample. The magnetic measurements were carried out on a vibrating sample magnetometer (VSM), and the measurement results indicate the reduction of the magnetization of the TiO<sub>2</sub> coated Mn–Zn ferrite nanoparticles compared with the uncoated ferrite nanoparticles. High coercivity also shows that the prepared uncoated and coated ferrite nanoparticles are not superparamagnetic.

© 2003 Elsevier B.V. All rights reserved.

*Keywords:* Mn–Zn ferrite nanoparticles; Core-shell structure; Titania-nanocoating

## 1. Introduction

A nanocomposite is a material that contains a reinforcement component in the form of one or more ultrafine phase with dimensions less than 100 nm. The nanocomposite approach has been used to improve various material properties including mechanical, chemical, structural, optical, and electrical/magnetic properties [1]. Manganese zinc ferrites are technologically important materials because of their high magnetic permeability and low core losses. These ferrites have widely used in

electronic applications such as transformers, chock coils, noise filters, recording heading etc. [2,3]. As an important magnetic material, nanosized Mn–Zn ferrites also can find many applications in biomedicine as magnetic carrier, such as bio-separation, enzyme and protein immobilization, magnetic resonance imaging (MRI), and so on [4]. For these applications, proper surface coating with biocompatible materials is necessary because of the possible appearance of metal elemental toxicities. Titania (TiO<sub>2</sub>) is an important inorganic material with good biocompatibility [5] and is not decomposed in organism. In present work, we prepared Mn–Zn ferrite nanoparticles and then capped them with a shell of anatase-structured titania. In addition, there is a growing interest in

\* Corresponding author. Tel.: +86-25-379-4960; fax: +86-25-361-9983.

E-mail address: [guning@seu.edu.cn](mailto:guning@seu.edu.cn) (N. Gu).

scientific aspects and practical applications of anatase-structured titania as a catalyst [6,7]. It is possible to increase the amount of exposed active centers and realize magnetic-separation of catalyst by coating titania on the surface of nanosized magnetic material [8].

Ferrites are commonly produced by a ceramic process involving high temperature solid state reactions between the constituent oxides/carbonate. The particles obtained by this process are rather large and non-uniform in size. In this work, stearic acid gel method was used to prepare Mn–Zn ferrite nanoparticles. The size of obtained particles is about 6 nm in diameter with a narrow size distribution.

Several different fabrication processes have been reported for titania nanocoating, including: hydrolysis of titanium *n*-butoxide (TBOT) in alcohol/water solution [9] or in reverse microemulsions [10], hydrolysis and precipitation of titanyl sulfate ( $\text{TiOSO}_4$ ) [11] and so on. In this work, titania nanocoating on Mn–Zn ferrite particles was prepared by hydrolysis of titanium (IV) chloride ( $\text{TiCl}_4$ ) onto Mn–Zn ferrite particle surface. To our knowledge, this titania nanocoating method has never been reported.

## 2. Experimental

### 2.1. Preparation of Mn–Zn ferrite nanoparticles

Mn–Zn ferrite ( $\text{Mn}_x\text{Zn}_{1-x}\text{Fe}_2\text{O}_4$ ) nanoparticles were prepared by following procedure. Measured amounts of  $\text{MnCO}_3$ ,  $\text{Zn}(\text{NO}_3)_2 \cdot 6\text{H}_2\text{O}$  and  $\text{Fe}(\text{NO}_3)_3 \cdot 9\text{H}_2\text{O}$  (molar ratio of Mn:Zn:Fe = 3:2:10) were grinded into powders, respectively, and then added to molten stearic acid in turn. The mixture was heated by oil bath at 120 °C and stirred for 3–4 h. After that a brown gel was obtained. The gel was cooled in air and grinded into powder. This powder was then washed with ethanol three times and dried at 100 °C. Finally, black magnetic Mn–Zn ferrite was obtained by heating at 450 °C for 1 h.

### 2.2. Preparation titania-coated Mn–Zn ferrite nanoparticles

Composite  $\text{Mn}_x\text{Zn}_{1-x}\text{Fe}_2\text{O}_4/\text{TiO}_2$  nanoparticles were obtained by following procedure. The obtained Mn–Zn ferrite of 100 mg was grinded into powders and then dispersed in 20 ml ethanol by ultrasonic wave. 0.5 ml of  $\text{TiCl}_4$  was added to the ethanol solution with vigorous stirring. After 25 min the solution was added to an aqueous solution of nitric acid (pH 1, 100 ml), and stirred for 30 min when a yellow sol was obtained. Proper amount of ammonia was then added to the sol with stirring until a brown precipitate was obtained when the pH of supernatant was about 8–9. The precipitate was collected by filtration and washed with deionized water for three times. Such obtained titania-coated Mn–Zn ferrite particles were dried at 100 °C in air for 24 h and then grinded into powder. A part of the powder was heated at 400 °C for 3 h.

### 2.3. Characterization

The dried samples ( $\text{Mn}_x\text{Zn}_{1-x}\text{Fe}_2\text{O}_4$  and  $\text{Mn}_x\text{Zn}_{1-x}\text{Fe}_2\text{O}_4/\text{TiO}_2$  powder obtained above) were analyzed for their composition, microstructure and magnetic properties. The element analysis was performed by energy dispersive X-ray spectroscopy (SEM-EDS, EDAX, PV9100). The structural property was determined by X-ray diffraction (XRD, Rigaku, D/Max-RA,) with  $\text{Cu K}_\alpha$  radiation ( $\lambda = 0.15418$  nm) and electronic diffraction (ED, JEOL, JEM-200CX). The crystallite size was measured using XRD linewidth based on Scherrer's formula [12]. Transmission electron microscopy (TEM, JEOL, JEM-200CX) was used at 200 kV to observe the morphology and particle size of the samples. For TEM observation, the powder samples were redispersed in ethanol and were sonicated for 20 min to obtain the better particle dispersion on carbon film covered copper grid. The magnetic measurements were carried out with a vibrating sample magnetometer (VSM, PARR, Model 4500).

### 3. Results and discussion

The ratio of Mn, Zn and Fe in the Mn–Zn ferrite obtained was determined to be 0.62:0.38:2 by SEM-EDS elemental analysis (Fig. 1), as expected by the preparation method. Consequently, the Mn–Zn ferrite obtained can be expressed as  $Mn_{0.62}Zn_{0.38}Fe_2O_4$ .

Fig. 2(c) shows XRD pattern of the Mn–Zn ferrite, presenting the characteristic peaks of cubic spinel structure. The broad ferrite peaks indicate very small crystallite size of the sample. The average crystallite diameter (ACD) of the Mn–Zn ferrite particles was determined from XRD linewidth of the (311) peak using the Scherrer's formula [12]:

$$ACD = 0.9\lambda / (\Delta w \times \cos \theta) \quad (1)$$

where  $\lambda$  is the X-ray wavelength,  $\theta$  the angle of Bragg diffraction, and  $\Delta w$  is the difference between the full-width at half-maximum (FWHM) and the instrumental broadening. The calculated ACD value is 6 nm in agreement with TEM results shown in Fig. 3. Fig. 3(a) shows dark-field TEM micrograph, which indicates the diameter of the Mn–Zn ferrite nanoparticles in the range of 4–9 nm. The arrow indicates particle aggregates. These aggregates are also seen obviously from bright-field TEM micrograph (Fig. 3(b)), with a size distribution of 10–20 nm.

Fig. 3(c) shows TEM micrograph of the prepared titania-coated Mn–Zn ferrite nanoparticles. It is clearly seen that the composite particles have larger size in the range of 30–100 nm as compared

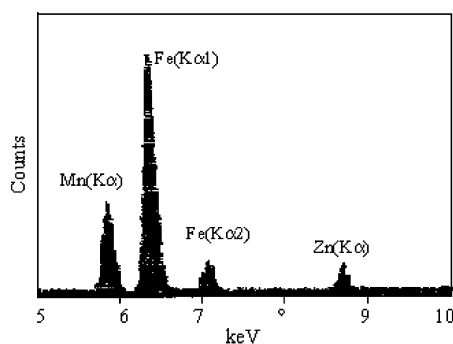


Fig. 1. SEM-EDS elemental analysis of Mn–Zn ferrite nanoparticles.

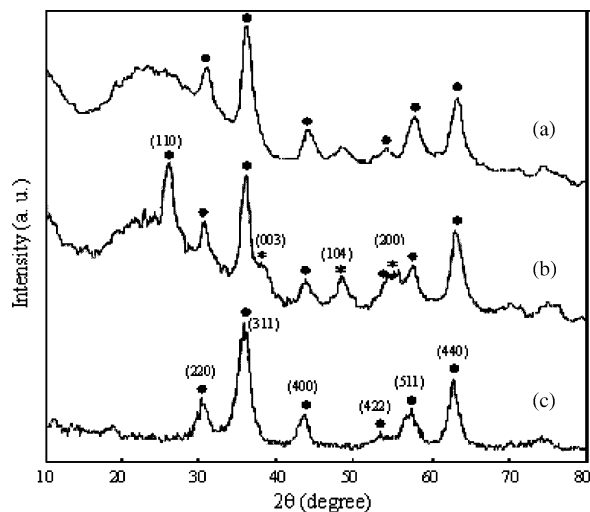


Fig. 2. XRD patterns of  $Mn_xZn_{1-x}Fe_2O_4$  nanoparticles (c) and  $Mn_xZn_{1-x}Fe_2O_4/TiO_2$  composite nanoparticles before (a) and after (b) annealing.

with the uncoated Mn–Zn ferrite nanoparticles or their aggregates, and the core-shell structure (dark Mn–Zn ferrite core with grey  $TiO_2$  shell) can be observed. The average  $TiO_2$  load in the composite particles was estimated to be 83% (wt.) according to SEM-EDS elemental analysis. The  $TiO_2$  coating layer has an anatase structure for the annealed titania-coated Mn–Zn ferrite sample, determined from XRD pattern in Fig. 2(b) where the peaks of (110), (003), (104) and (200) are the characteristic peaks of anatase structural  $TiO_2$  [12]. Fig. 2(a) also gives XRD pattern of the titania-coated Mn–Zn ferrite sample before annealing, where no characteristic peaks of  $TiO_2$  are observed. In addition, as expected, XRD peaks of the Mn–Zn ferrite cores remain unchanged as compared with Fig. 2(c), suggesting their spinel structure.

For the Mn–Zn ferrite nanoparticles, a typical ED ring pattern of spinel structure is also shown in Fig. 3(d). Fig. 3(e) gives ED pattern of the  $TiO_2$  coated Mn–Zn ferrite nanoparticles. In contrast, the characteristic diffraction rings of  $TiO_2$  appear in the coated sample, as indicated with arrows, attributed to (110) and (104) lattice faces of anatase  $TiO_2$ . According to ED pattern, the  $d$ -spacing can be calculated in the following equation [13]:

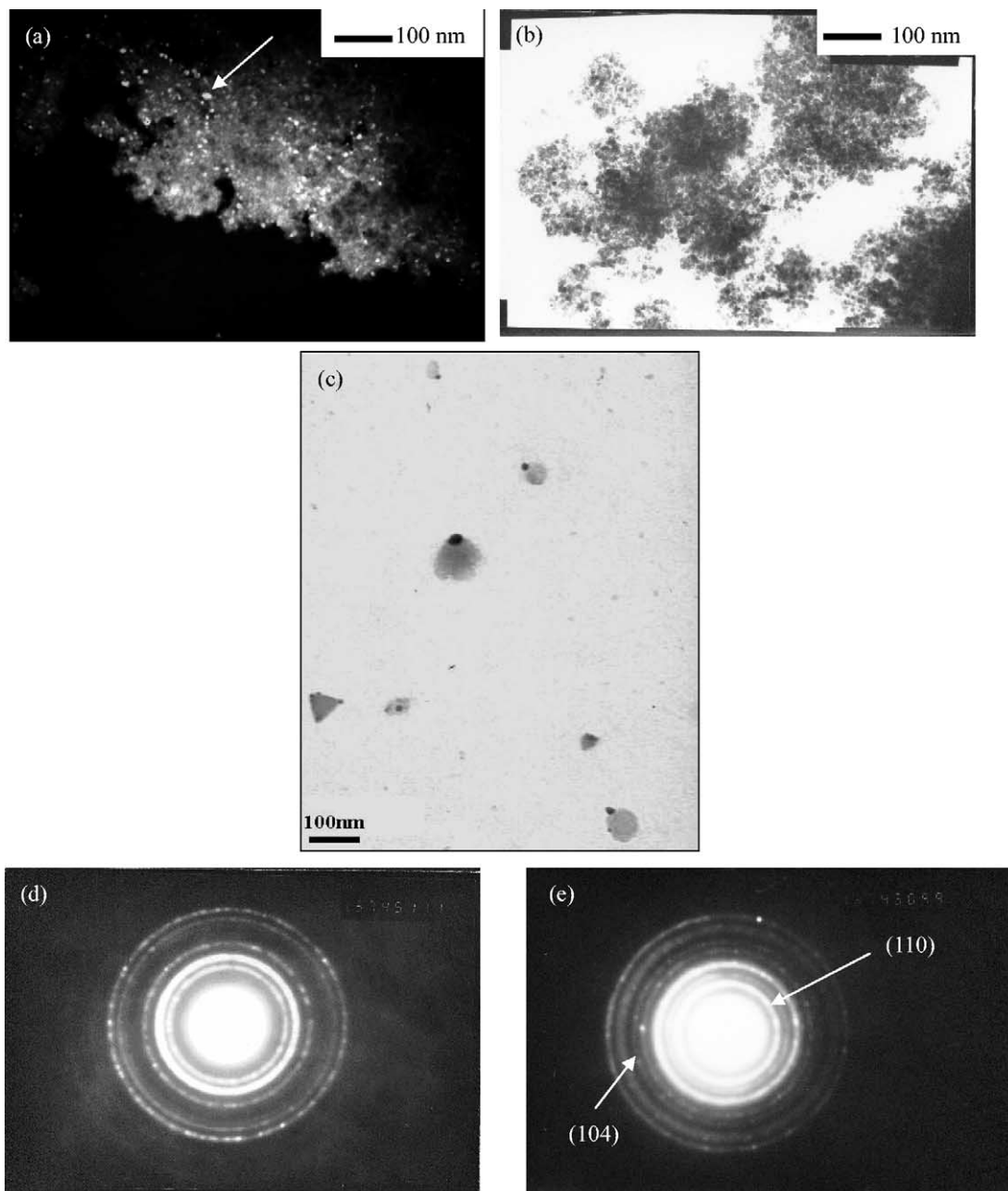


Fig. 3. Dark-field (a) and light-field (b) TEM micrograph of Mn-Zn ferrite nanoparticles, TEM micrograph of TiO<sub>2</sub> coated Mn-Zn ferrite nanoparticles (c), ED ring pattern of Mn-Zn ferrite nanoparticles (d) and TiO<sub>2</sub> coated Mn-Zn ferrite nanoparticles (e).

$$d_{ED} = L\lambda/R \quad (2)$$

where  $L$  is the distance (137 cm) between the sample and the film,  $R$  the radius of the diffraction

ring and  $\lambda$  is the wavelength (0.0251 Å) of electron beam applied. Detailed calculation results are shown in Table 1. Table 1 gives simultaneously  $d_{XRD}$  values calculated from XRD pattern using

Table 1  
*d*-spacing calculated from ED and XRD patterns for Mn–Zn ferrite and TiO<sub>2</sub>

	<i>d</i> <sub>ED</sub>	<i>d</i> <sub>XRD</sub>	<i>d</i> <sub>theory</sub>	( <i>hkl</i> )
Ferrite core (spinel)	2.87	2.94	2.99	(220)
	2.50	2.53	2.55	(311)
	2.08	2.08	2.11	(400)
	1.70	1.71	1.72	(422)
	1.60	1.61	1.63	(511)
	1.48	1.48	1.49	(440)
TiO <sub>2</sub> shell (anatase)	3.52, 1.91	3.47, 1.90	3.52, 1.89	(110), (104)

Bragg formula. A good agreement is found for two calculation results. Compared with theoretical values, the reduction of *d*-spacing is observed due to lattice constrictions for nanosized particles [13].

The titania-coated Mn–Zn ferrite nanoparticles have been obtained as demonstrated above. Possibly, we give their formation process, as follows (Fig. 4). As described by the preparation method, the formation of a monolayer of –OTi(OEt)<sub>3</sub> is thought to be helpful for further inducing the formation of TiO<sub>2</sub> shell. Finally obtained composite nanoparticle colloid has high stability. The dried powder also has higher resolvability in water than the uncoated Mn–Zn ferrite nanoparticles. This is useful for biological applications in the form of magnetic fluid.

The magnetic properties of the uncoated and coated Mn–Zn ferrite nanoparticle powder were measured by VSM, as shown in Fig. 5. From VSM experiments, the magnetic parameters such as saturation magnetization (*M*<sub>s</sub>), coercivity (*H*<sub>c</sub>) and remnant magnetization (*M*<sub>r</sub>) were given in Table 2. In contrast, *M*<sub>s</sub> of the TiO<sub>2</sub> coated Mn–

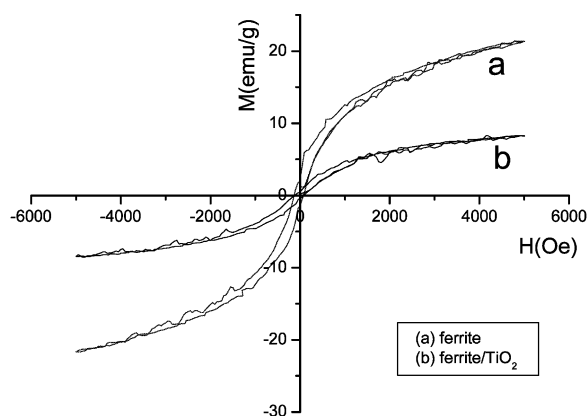


Fig. 5. Magnetization vs. applied magnetic field for the uncoated and coated Mn–Zn ferrite nanoparticle powder with TiO<sub>2</sub>.

Zn ferrite decreases, attributed mainly to the contribution of the volume of the non-magnetic coating layer to the total sample volume. In addition, the non-magnetic coating layer can be considered as a magnetically dead layer at the surface, thus affecting the uniformity or magnitude of magnetization due to quenching of surface

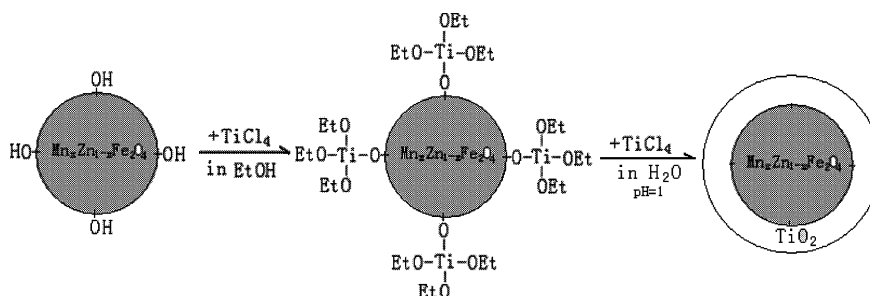


Fig. 4. The formation procedure of the titania coated Mn–Zn ferrite nanoparticles.

Table 2  
Magnetic parameters of the uncoated and coated Mn–Zn ferrite with TiO<sub>2</sub>

Sample	Ms (emu g <sup>-1</sup> )	Hc (Oe)	Mr (emu g <sup>-1</sup> )
Ferrite	21.3	109.6	1.79
Ferrite/TiO <sub>2</sub>	8.2	113.5	0.43

moments [14]. Note that, although the particles are nanoscale, they are not superparamagnetic as confirmed from the high Hc values. Moreover, these values are much larger than that of bulk ferrites (0.1–1 Oe), in agreement with the literature reported [15].

In summary, the titania-coated Mn–Zn ferrite nanoparticles, A novel nanocomposite material, have been obtained, and their composition, morphology, microstructural and magnetic properties have been characterized.

### Acknowledgements

This work was supported by the National Natural Science Foundation of China (No. 60171005) and the High Technology Research Subject of Jiangsu Province in China (BG2001006). We are also very grateful to Professor Hong Jian-min of Center of Analysis and

Test, Nanjing University for his helping in TEM experiments.

### References

- [1] A.J. Ruys, Y. Mai, *Mater. Sci. Eng. A* 265 (1999) 202–207.
- [2] K.I. Arshak, A. Ajina, D. Egan, *Microelectron. J.* 32 (2001) 113–116.
- [3] X.D. Tong, B. Xue, Y. Sun, *Biotech. Prog.* 17 (2001) 134–139.
- [4] A. Kondo, H. Fukuda, *J. Ferment. Bioeng.* 84 (1997) 337–341.
- [5] D.B. Haddow, P.F. James, R. Vannoort, *J. Mater. Sci. Mater. Med.* 7 (1996) 255.
- [6] M.R. Hoffmann, S.T. Martin, W. Choi, D. Bahnemann, *Chem. Rev.* 95 (1995) 69–96.
- [7] K.Y. Jung, S.B. Park, *J. Photochem. Photobiol. A* 127 (1999) 117–122.
- [8] D. Beydoun, R. Amal, G.K.C. Low, S. McEvoy, *J. Phys. Chem. B* 104 (2002) 4387–4396.
- [9] X. Fu, S. Qutubuddin, *Coll. Surf. A* 178 (2001) 151–156.
- [10] X. Fu, S. Qutubuddin, *Coll. Surf. A* 179 (2001) 65–70.
- [11] F. Hiroshi, H. Yukiko, Y. Michichiro, A. JP 06154620, 1994.
- [12] K. Mandal, S.P. Mandal, P. Agudo, M. Pal, *Appl. Surf. Sci.* 182 (2001) 386.
- [13] M. Ma, Y. Zhang, W. Yu, H.Y. Shen, H.Q. Zhang, N. Gu, *Coll. Surf. A* 212 (2003) 219–226.
- [14] R. Kaiser, G. Miskolczy, *J. Appl. Phys.* 41 (1970) 1064.
- [15] C. Rath, K.K. Sahu, S. Anand, S.K. Date, N.C. Mishra, R.P. Das, *J. Magn. Magn. Mater.* 202 (1999) 77–84.